Proceedings of the Royal Society B

Electronic supplementary material for spatial reciprocity in the evolution of cooperation

Qi Su[1,2], Aming Li[3,4,1], Long Wang[1,*], and H. Eugene Stanley[2,†]

[1] *Center for Systems and Control, College of Engineering, Peking University, Beijing 100871, CN*

[2] *Center for Polymer Studies, Department of Physics, Boston University, Boston, Massachusetts 02115, USA*

[3] *Chair of Systems Design, ETH Zürich, Weinbergstrasse 56/58, Zürich CH-8092, CH*

[4] *Department of Zoology, University of Oxford, Oxford, Oxfordshire OX1 3PS, UK*

∗ *E-mail: longwang@pku.edu.cn*

† *E-mail: hes@bu.edu*

DOI: 10.1098/rspb.2019.0041

1 Supplementary figures

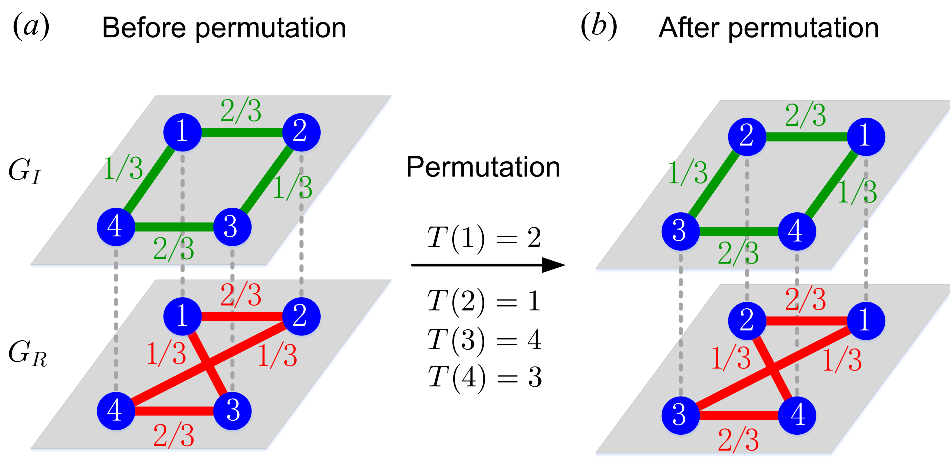

Figure S1. An illustrative description of joint transitive graphs. G_I and G_R are joint transitive graphs if for every pair of nodes $i, j \in V$, there is a permutation T of V such that $T(i) = j$ and meanwhile $d_{T(m)T(n)} = d_{mn}$, $e_{T(m)T(n)} = e_{mn}$ for every pair of m, n [1, 2, 3]. Here we check the node transitivity of a pair of simple graphs. (*a*) Graphs before permutation. (*b*) Graphs after permutation. For a pair of nodes 1 and 2, a permutation can be $T(1) = 2$, $T(2) = 1$, $T(3) = 4$, and $T(4) = 3$. In the meanwhile, $d_{13} = d_{T(1)T(3)}$, $e_{13} = e_{T(1)T(3)}$, etc. Thus, graphs in (*a*) are joint transitive. Roughly speaking, graphs are joint transitive if they look the same from any node [3]. For example, in (*a*), when moving a player from 1 to 2, it can not tell whether or not being moved in terms of global configuration information (both edge connections and edge weights).

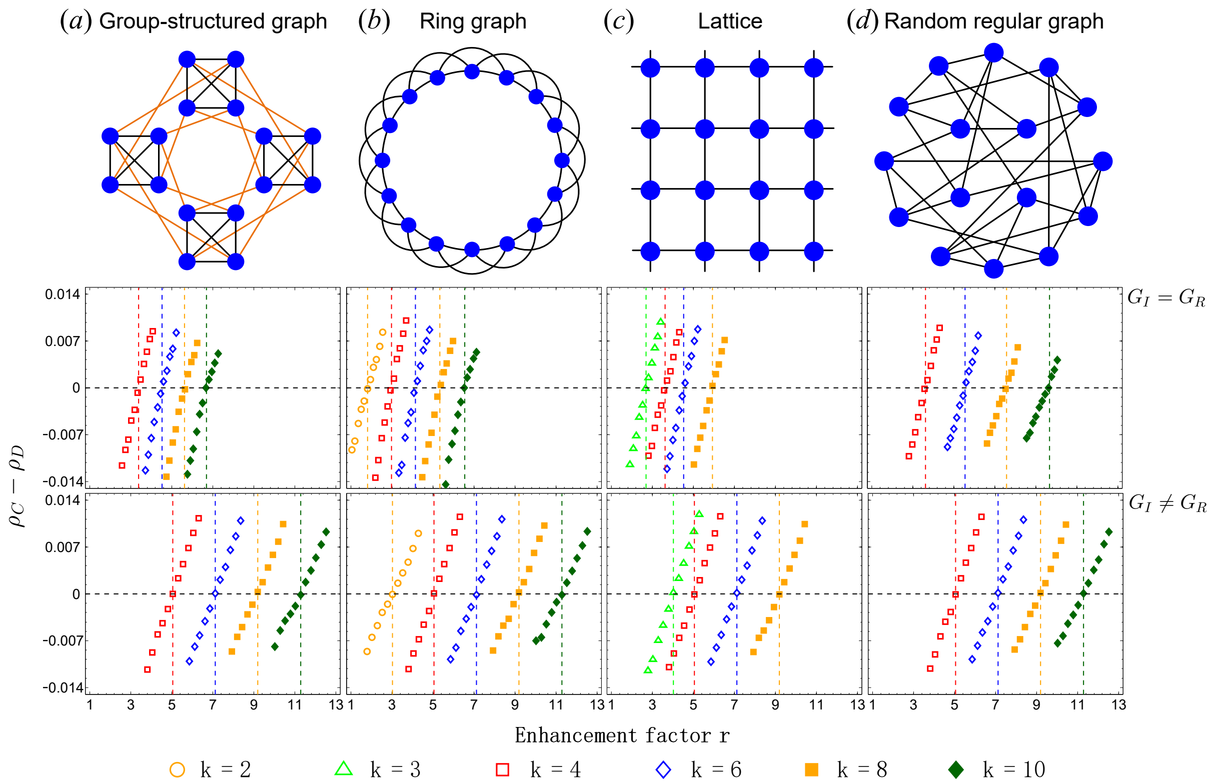

Figure S2. Critical enhancement factor r^* for $\rho_C > \rho_D$. The analytical critical enhancement factor r^* for fixation probability $\rho_C > \rho_D$ is in good agreement with computer simulations. Here we take unweighted G_I and G_R with $k_I = k_R = k$. The first row illustrates three types of transitive graphs (*a*-*c*) and a type of non-transitive graph (*d*). The second and third rows present results for symmetric G_I and G_R ($G_I = G_R$), and asymmetric G_I and G_R ($G_I \neq G_R$), respectively. Both G_I and G_R used in row $G_I = G_R$ are graphs illustrated in the first row. In row $G_I \neq G_R$, G_I corresponds to the graph shown in the first row and G_R is a random regular graph. For group-structured graphs, to ensure that sizes of all groups are equal, sizes of graphs vary slightly for different k, namely, $N = 402$ for $k = 4$, 400 for $k = 6$, 399 for $k = 8$, and 405 for $k = 10$, respectively. For other graphs, the size is $N = 400$. ρ_C (ρ_D) is determined by the fraction of runs where cooperators (defectors) reach fixation out of 10^5 runs under weak selection, $\delta = 0.01$. We simulate each type of graphs for different degrees ranging from $k = 2$ to $k = 10$. The vertical dashed lines mark the analytical value of r^*.

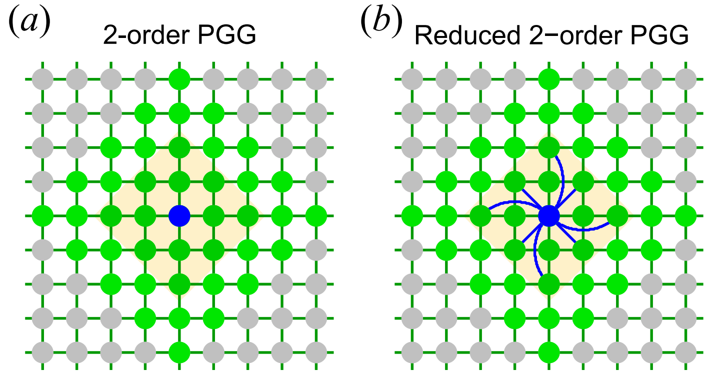

Figure S3. Reduction of 2-order PGG on graphs to the conventional public goods game on graphs. Only the interaction graph is presented. (*a*) 2-order PGG on graphs. The focal player (blue filled circle) participates in all games centred on itself, first-order and second-order neighbours. Its interaction partners include all players within a 4-step walk from the focal player, highlighted by green circles. Mathematically, any l-order ($l > 1$) PGG could be reduced to a conventional PGG by amending the interaction graph (see §2). First, linking all nodes within a l-step walk from the node occupied by the focal player to the node occupied by the focal player. Note that multiple edges are not allowed. Second, recording the number of participants in an original l-order PGG, given by $\tilde{k}+1$, and revising all edge weights in new generated interaction graph to $1/\tilde{k}$. (*b*) Reduced 2-order PGG on graphs. A 2-order PGG is reduced to a conventional PGG by connecting all second-order neighbours to the focal player and adjusting all edge weights from $1/4$ to $1/12$ ($\tilde{k} = 12$). The evolutionary dynamics remains unchanged after the reduction.

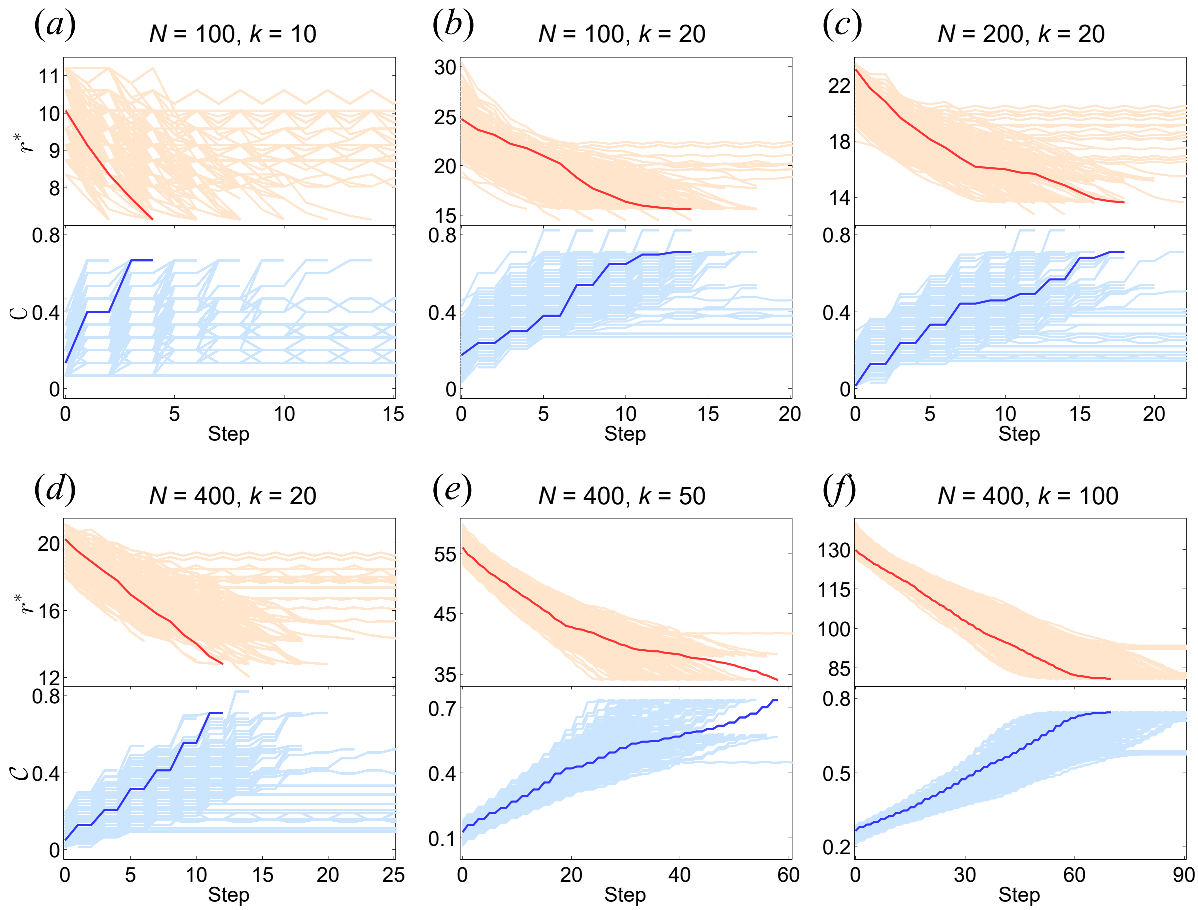

Figure S4. Enhancement of spatial reciprocity. The spatial reciprocity is enhanced as the adjustment of social ties based on a simple algorithm. The details are: each player rewires interaction edges to players with more interactions; each player rewires dispersal edges to players with more interactions. Note that multiple edges are not allowed. The algorithm runs in 1000 randomly generated and initially symmetric transitive graphs ($k_I = k_R = k$). Critical enhancement factor r^* and clustering coefficient $\mathcal{C}$ in different steps are respectively shown in the upper and lower panels. Bright red and blue lines illustrate a representative evolving process. Parameters: $N = 100, k = 10$ (*a*); $N = 100, k = 20$ (*b*); $N = 200, k = 20$ (*c*); $N = 400, k = 20$ (*d*); $N = 400, k = 50$ (*e*); $N = 400, k = 100$ (*f*).

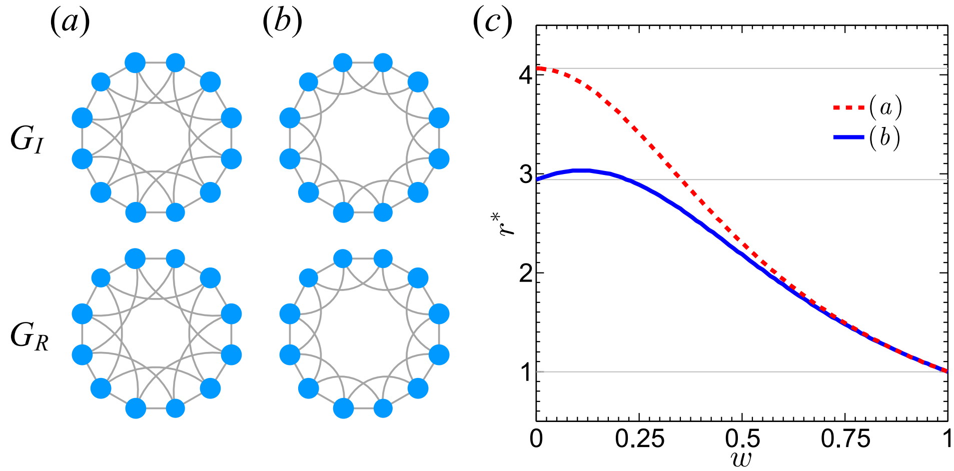

Figure S5. **Sufficiently large participation frequency in self-centred games w promotes cooperation**. (a) Spatial structure without structural clusters. (b) Spatial structure with structural clusters. All edge weights are $1/4$. r^* is shown as a function of w.

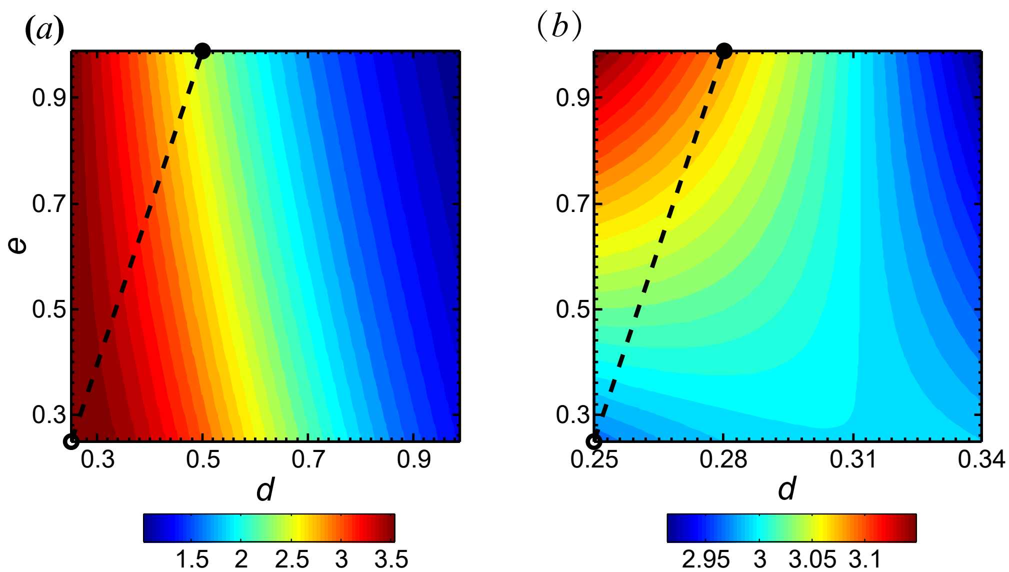

Figure S6. **Promotive and inhibitive effects of strong social ties**. The spatial structure corresponding to (a) is the one shown in figure 4(a) in the main text. The spatial structure corresponding to (b) is the one shown in figure 4(b) in the main text. r^* as a function of d and e. Here $d = 0.3e + 0.175$ in (a), $d = 0.04e + 0.24$ in (b), and $w = 1/5$. Strong social ties always lower the barrier for the evolution of cooperation in structures with no structural clusters (a) while might hinder cooperation in the presence of structural clusters (b).

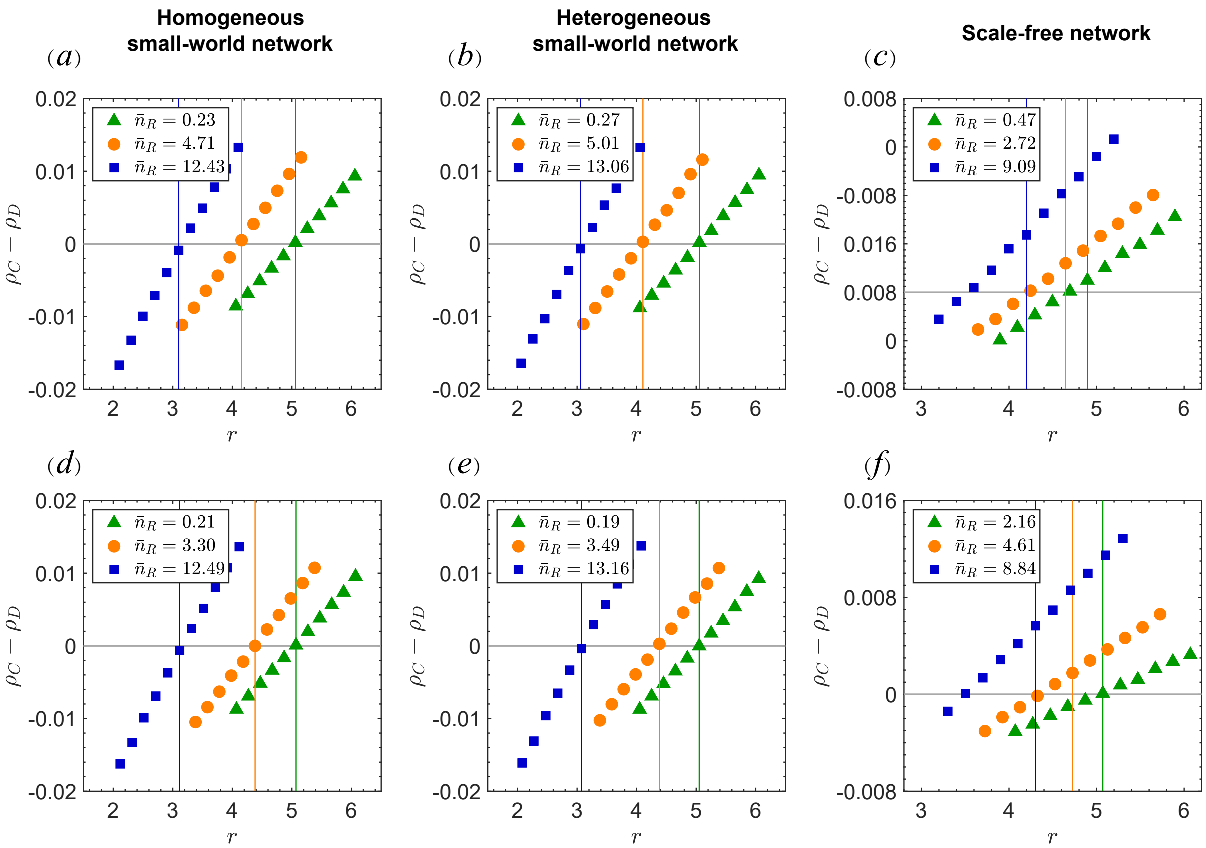

Figure S7. $\bar{n}_R$ **is positively correlated to the strength of spatial reciprocity**. This extends our finding in Eq (3.3) in the main text to practical social networks. Both the interaction graph (G_I) and the dispersal graph (G_R) are homogeneous small-world networks in panels (*a*) and (*d*), heterogeneous small-world networks in panels (*b*) and (*e*), and scale-free networks in panels (*c*) and (*f*). In panels (*a*-*c*), we use 'edge swapping' pattern to get pairs of interaction and strategy dispersal networks with tuneable $\bar{n}_R$. We take $h = 2400$, $h = 400$, and $h = 0$ to get three pairs of networks with different $\bar{n}_R$ (*a*-*c*). In panels (*d*-*f*), we use 'node rearranging' pattern to get pairs of interaction and strategy dispersal networks with tuneable $\bar{n}_R$. We take $\hat{N} = 400$, $\hat{N} = 200$, and $\hat{N} = 0$ to get three pairs of networks with different $\bar{n}_R$ (*d*-*f*). Dots represent the simulation data and the cross points of dots and horizontal lines are the critical enhancement factor r^*. The vertical lines are analytical results given by Eq (3.2) in the main text (θ is calculated based on averaged values of n_I, n_R, average degree k_I in G_I and k_R in G_R). We take $N = 400$, $k_I = 4$, $k_R = 4$. ρ_C (ρ_D) is determined by the fraction of runs where a cooperator (defector) reaches fixation out of 10^6 runs under weak selection, $\delta = 0.01$. Other parameter values: the times of swapping edges in generating a homogeneous network are 40 (see Ref [4]) (*a*); the rewiring probability in generating a Watts-Strogatz heterogeneous small-world network is 0.05 (see Ref [5]) (*b*).

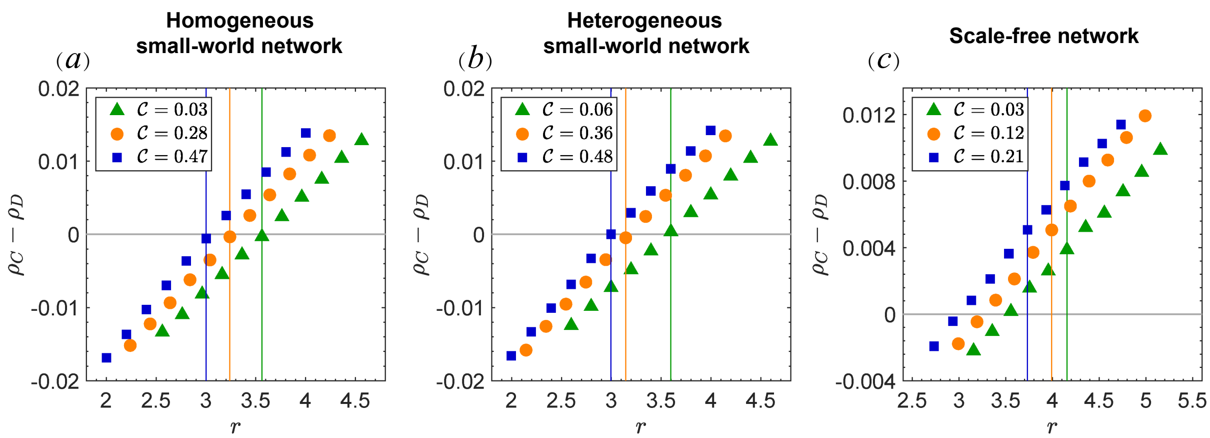

Figure S8. **Structural clusters promote the evolution of cooperation**. Here we take a pair of symmetric networks for interaction and strategy dispersal. We build the homogeneous small-world network based on the algorithm given in Ref [4]. Swapping edges for 400, 80 and 8 times leads to a clustering coefficient of $\mathcal{C}=0.03$, $\mathcal{C}=0.28$ and $\mathcal{C}=0.47$, respectively. We build the Watts-Strogatz heterogeneous small-world network based on the algorithm given in Ref [5]. The edge rewiring probability of 0.5, 0.1 and 0.01 leads to a clustering coefficient of $\mathcal{C}=0.06$, $\mathcal{C}=0.36$ and $\mathcal{C}=0.48$, respectively. We build a scale-free network with tunable clustering coefficients based on the algorithm given in Ref [6]. The triad formation probability of 0, 0.5 and 0.9 leads to a clustering coefficient of $\mathcal{C}=0.03$, $\mathcal{C}=0.12$ and $\mathcal{C}=0.21$, respectively. Dots represent the simulation data and the cross points of dots and horizontal lines are the critical enhancement factor r^*. The vertical lines are analytical results given by Eq (3.2) in the main text (θ is calculated based on the average value of n_I, n_R, average degree k_I in G_I and k_R in G_R). We take $N=400$, $k_I=4$, $k_R=4$. ρ_C (ρ_D) is determined by the fraction of runs where a cooperator (defector) reaches fixation out of 10^6 runs under weak selection, $\delta=0.01$.

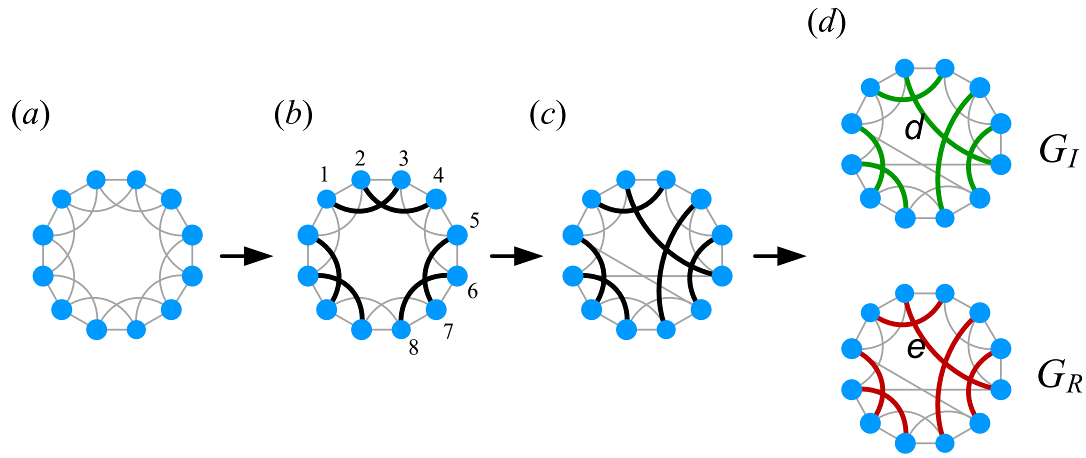

Figure S9. **Generating a homogeneous small-world network with strong social ties**. Here we present how to incorporate strong social ties in a homogeneous small-world network with node degree 4 and meanwhile make sure that each node has a strong social tie. Networks with other degrees can be built analogously. (*a*) Generate a ring graph of size N with node degree 4 (we require that N can be divided by 4). (*b*) Four consecutive nodes form a group $(1, 2, 3, 4; 5, 6, 7, 8; \cdots)$; in each group cross connections are marked as 'thick' edges (1 and 3, 2 and 4, 5 and 7, 6 and 8, $\cdots$) and other connections are marked as 'thin' edges. (*c*) Randomly select two 'thick' edges or two 'thin' edges and swap the ends of the two edges if no duplicate edges arise; repeat the edge swapping for h times and produce network G; (*d*) Get two copies of G, one for the interaction graph G_I, where 'thick' edges are endowed with weight d and 'thin' edges with weight $(1-d)/3$, one for the strategy dispersal graph G_R where 'thick' edges are endowed with weight e and 'thin' edges with weight $(1-e)/3$. When both d and e are larger than $1/4$, joint 'thick' edges in G_I and G_R form strong social ties.

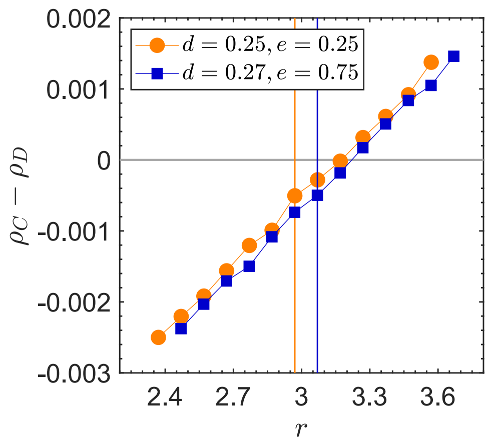

Figure S10. **Strong social ties might inhibit the evolution of cooperation**. We generate a class of homogeneous small-world networks with strong social ties based on the algorithm illustrated in figure S9. We take $h = 40$ [see step (c) in figure S9]. The setting with $d = 0.25$ and $e = 0.25$ corresponds to the spatial structure without strong social ties. The setting with $d = 0.27$ and $e = 0.75$ corresponds to the spatial structure with strong social ties. Dots represent the simulation data and the cross points of dots and horizontal lines are the critical enhancement factor r^*. The vertical lines are analytical results given by Eq (3.2) in the main text (θ is calculated based on the average value of n_I, n_R, average degree k_I in G_I and k_R in G_R). We take $N = 400$, $k_I = 4$, $k_R = 4$. ρ_C (ρ_D) is determined by the fraction of runs where a cooperator (defector) reaches fixation out of 10^6 runs under weak selection, $\delta = 0.01$.

§1. An exact condition for $\rho_C > \rho_D$ on weighted and asymmetric graphs

Here we take the method of identity by descent to derive the condition for cooperation to be favoured over defection. This method has been used to investigate two-player games on graphs (see Ref. [3] for more details). We describe the evolution process by an evolutionary Markov chain. Each state S is written as a string $(s_1, \cdots, s_N)$, where $s_i \in \{0, 1\}$ denotes the strategy taken by the player currently occupying node i (called player i). $s_i = 1$ represents cooperation and $s_i = 0$ means defection. Let b_i denote probability that player i reproduces in a given state and d_i denote the probability that player i is replaced. Cooperation is favoured over defection if the fixation probability of cooperation ρ_C is larger than the fixation probability of defection ρ_D. In the limit of low mutation ($\mu \to 0$) and in joint transitive graphs, the condition $\rho_C > \rho_D$ is equivalent to the condition [3]

$$\left\langle \frac{\partial}{\partial \delta}(b_1 - d_1) \right\rangle_{\substack{\delta=0\\ s_1=1}} > 0, \tag{S1}$$

where $\langle \cdot \rangle_{\substack{\delta=0\\ s_1=1}}$ denotes that the average over the stationary distribution of the neutral drift process (δ is the intensity of selection), conditioned on player 1 taking cooperation ($s_1 = 1$). Let f_i denote i's accumulative payoffs from all interactions and $F_i = 1 - \delta + \delta f_i$ denote the transformation of payoff to fitness.

We consider four update rules:

1. Birth-death(BD) [7]: A player such as i is selected with probability proportional to F_i to reproduce. Its offspring occupies a neighbouring node j with probability proportional to e_{ij}.

2. Death-birth(DB) [7]: A player such as i is selected with uniform probability to die. A random neighbour such as j is selected to reproduce with probability proportional to $e_{ji}F_j$ and its offspring occupies i.

3. Pairwise comparison(PC) [8]: A player i is selected with uniform probability to be potentially replaced. A random neighbour j is selected with probability e_{ji}. Then j reproduces an offspring to reproduce i with $P(F_j - F_i) = (1 + e^{-(F_j - F_i)})^{-1}$. Otherwise, no dispersal event happens.

4. Imitation(IM) [7]: A player i is selected with uniform probability to be potentially replaced. A random player j in i's neighbourhood (including i) is selected with probability proportional to F_j.

Taking above rules into equation (S1), we get

BD:

$$\left\langle \frac{\partial}{\partial \delta}\left(\frac{F_1}{\sum_{l\in V} F_l} - \sum_{i\in V} \frac{e_{i1}F_i}{\sum_{l\in V} F_l} \right) \right\rangle_{\substack{\delta=0\\ s_1=1}} > 0 \Leftrightarrow \langle f_1 \rangle_{\substack{\delta=0\\ s_1=1}} - \left\langle \sum_{i\in V} e_{i1} f_i \right\rangle_{\substack{\delta=0\\ s_1=1}} > 0; \tag{S2}$$

DB:

$$\left\langle \frac{\partial}{\partial \delta}\left(\frac{1}{N}\sum_{i\in V} \frac{e_{i1}F_1}{\sum_{l\in V} e_{il}F_l} - \frac{1}{N} \right) \right\rangle_{\substack{\delta=0\\ s_1=1}} > 0 \Leftrightarrow \langle f_1 \rangle_{\substack{\delta=0\\ s_1=1}} - \left\langle \sum_{i,l\in V} e_{i1} e_{il} f_l \right\rangle_{\substack{\delta=0\\ s_1=1}} > 0; \tag{S3}$$

PC:

$$\left\langle \frac{\partial}{\partial \delta} \left(\frac{1}{N} \sum_{i \in V} \frac{e_{i1}}{1+e^{-(F_1-F_i)}} - \frac{1}{N} \sum_{i \in V} \frac{e_{i1}}{1+e^{-(F_i-F_1)}} \right) \right\rangle_{\substack{\delta=0 \\ s_1=1}} > 0$$

$$\Leftrightarrow \langle f_1 \rangle_{\substack{\delta=0 \\ s_1=1}} - \left\langle \sum_{i \in V} e_{i1} f_i \right\rangle_{\substack{\delta=0 \\ s_1=1}} > 0; \tag{S4}$$

IM:

$$\left\langle \frac{\partial}{\partial \delta} \left(\frac{1}{N} \sum_{i \in N_1^R} \frac{F_1}{\sum_{l \in N_i^R} F_l + F_i} - \frac{1}{N} \frac{\sum_{l \in N_1^R} F_l}{\sum_{l \in N_1^R} F_l + F_1} \right) \right\rangle_{\substack{\delta=0 \\ s_1=1}} > 0$$

$$\Leftrightarrow \langle f_1 \rangle_{\substack{\delta=0 \\ s_1=1}} - \frac{2}{k_R(k_R+2)} \left\langle \sum_{i \in N_1^R} f_i \right\rangle_{\substack{\delta=0 \\ s_1=1}} - \frac{1}{k_R(k_R+2)} \left\langle \sum_{i \in N_1^R} \sum_{l \in N_i^R} f_l \right\rangle_{\substack{\delta=0 \\ s_1=1}} > 0. \tag{S5}$$

Above, N_i^R is the set of i's adjacent nodes in dispersal graph G_R. $\langle f_1 \rangle_{\substack{\delta=0 \\ s_1=1}}$ denotes the average payoff of player 1. $\left\langle \sum_{i \in V} e_{i1} f_i \right\rangle_{\substack{\delta=0 \\ s_1=1}}$ and $\left\langle \sum_{i \in N_1^R} f_i \right\rangle_{\substack{\delta=0 \\ s_1=1}} / k_R$ denote the expected payoff of a player that is at the end of an one-step random walk from the node occupied by player 1. $\left\langle \sum_{i,l \in V} e_{i1} e_{il} f_l \right\rangle_{\substack{\delta=0 \\ s_1=1}}$ and $\left\langle \sum_{i \in N_1^R} \sum_{l \in N_i^R} f_l \right\rangle_{\substack{\delta=0 \\ s_1=1}} / k_R^2$ denote the expected payoff of a player that is at the end of a two-step random walk from the node occupied by player 1.

Before taking the identity-by-descent (IBD) methods to derive the assortment of strategies at neutrality, we define a $(n$,$m)$-random walk to be a random walk with n steps using the weights $\{d_{ij}\}$ of G_I, and m steps using the weights $\{e_{ij}\}$ of G_R. $p^{(n,m)}$ denotes the probability that such a random walk terminates at its starting node. $s^{(n,m)}$ denotes the probability that a player at the end of an (n,m)-random walk from the node occupied by player 1 takes cooperation. In the low-mutation limit, we get [3]

$$s^{(n,m)} - s^{(n,m+1)} = \frac{\mu}{2}(Np^{(n,m)} - 1) + \mathcal{O}(\mu^2), \tag{S6}$$

where μ means the mutation rate. Let $f^{(n,m)}$ denote the expected payoff that a player at the end of a $(n$,$m)$-random walk from player 1 gets. Equations (S2), (S3), (S4) and (S5) are respectively equivalent to $f^{(0,0)} > f^{(0,1)}$ (BD), $f^{(0,0)} > f^{(0,2)}$ (DB), $f^{(0,0)} > f^{(0,1)}$ (PC), and $f^{(0,0)} > (2f^{(0,1)} + k_R f^{(0,2)})/(k_R+2)$ (IM). Combining our definition about public goods games on weighted graphs (see Model section in the main text), we have

$$\begin{aligned} f^{(n,m)} &= rw[(1-w)s^{(n+1,m)} + ws^{(n,m)}] - ws^{(n,m)} \\ &\quad + r(1-w)[(1-w)s^{(n+2,m)} + ws^{(n+1,m)}] - (1-w)s^{(n,m)} \\ &= r(1-w)^2 s^{(n+2,m)} + 2rw(1-w)s^{(n+1,m)} + (rw^2-1)s^{(n,m)} \end{aligned} \tag{S7}$$

The first and second terms following the first equality are allocated benefits and corresponding investment in the self-centred game. The third and fourth terms are allocated benefits and corresponding investment in games centred on first-order neighbours. We call player j is an l_{th}-order neighbour of player i if and only if player j can reach node i by a $l-$step walk.

Birth-death (BD)/Pairwise comparison (PC).

Substituting equation (S7) into $f^{(0,0)} > f^{(0,1)}$, we get

$$\begin{aligned} f^{(0,0)} - f^{(0,1)} =& r(1-w)^2(s^{(2,0)} - s^{(2,1)}) + 2rw(1-w)(s^{(1,0)} - s^{(1,1)}) \\ &+ (rw^2-1)(s^{(0,0)} - s^{(0,1)}) \end{aligned} \tag{S8}$$

Substituting equation (S6) into equation (S8), we have

$$\begin{aligned} & r\left\{N[(1-w)^2p^{(2,0)} + 2w(1-w)p^{(1,0)} + w^2p^{(0,0)}] - 1\right\} - (Np^{(0,0)} - 1) > 0 \\ \Longleftrightarrow & r > \frac{Np^{(0,0)} - 1}{N[(1-w)^2p^{(2,0)} + 2w(1-w)p^{(1,0)} + w^2p^{(0,0)}] - 1} \\ \Longleftrightarrow & r > \frac{N-1}{N[(1-w)^2\kappa^{-1} + w^2] - 1} \equiv r^*, \end{aligned} \tag{S9}$$

where $\kappa = (\sum_j d_{ij}^2)^{-1}$ respresents the Simpson degree [9]. In the unweighted interaction graph, κ equals to the node degree k_I. We get the third term since there are no self-loops in both interaction and dispersal graphs, i.e., $p^{(0,1)} = 0, p^{(1,0)} = 0$. Results for PC and BD update rules are identical.

Death-birth (DB).

Substituting equation (S7) into $f^{(0,0)} > f^{(0,2)}$, we get

$$\begin{aligned} f^{(0,0)} - f^{(0,2)} =& r(1-w)^2(s^{(2,0)} - s^{(2,2)}) + 2rw(1-w)(s^{(1,0)} - s^{(1,2)}) \\ &+ (rw^2-1)(s^{(0,0)} - s^{(0,2)}) \end{aligned} \tag{S10}$$

Substituting equation (S6) into equation (S10), we have

$$\begin{aligned} & r\{N[(1-w)^2(p^{(2,0)} + p^{(2,1)}) + 2w(1-w)(p^{(1,0)} + p^{(1,1)}) + w^2(p^{(0,0)} + p^{(0,1)})] - 2\} \\ & - [N(p^{(0,0)} + p^{(0,1)}) - 2] > 0 \\ \Longleftrightarrow & r > \frac{N(p^{(0,0)} + p^{(0,1)}) - 2}{N[(1-w)^2(p^{(2,0)} + p^{(2,1)}) + 2w(1-w)(p^{(1,0)} + p^{(1,1)}) + w^2(p^{(0,0)} + p^{(0,1)})] - 2} \\ \Longleftrightarrow & r > \frac{N-2}{N[(1-w)^2\kappa^{-1} + w^2 + 2w(1-w)p^{(1,1)} + (1-w)^2p^{(2,1)}] - 2} \equiv r^*. \end{aligned} \tag{S11}$$

Imitation (IM).

Substituting equation (S7) into $f^{(0,0)} > (2f^{(0,1)} + k_Rf^{(0,2)})/(k_R+2)$, we get

$$f^{(0,0)} - \frac{2}{k_R+2}f^{(0,1)} - \frac{k_R}{k_R+2}f^{(0,2)} = \frac{2}{k_R+2}(f^{(0,0)} - f^{(0,1)}) + \frac{k_R}{k_R+2}(f^{(0,0)} - f^{(0,2)}) \tag{S12}$$

Substituting equation (S6) into equation (S12), we have

$$r > \frac{N(k_R+2) - 2(k_R+1)}{N[(1-w)^2k_I^{-1}(k_R+2) + w^2(k_R+2) + 2w(1-w)k_Rp^{(1,1)} + k_R(1-w)^2p^{(2,1)}] - 2(k_R+1)} \equiv r^*. \tag{S13}$$

In joint transitive graphs, $p^{(1,1)} = \sum_j d_{ij} e_{ji}$ and $p^{(2,1)} = \sum_{j,l} d_{ij} d_{jl} e_{li}$, which do not depend on $i \in V$ due to node-transitivity. For non-transitive graphs like random regular graphs, we approximate $p^{(1,1)}$ and $p^{(2,1)}$ by $\sum_{i,j} d_{ij} e_{ji}/N$ and $\sum_{i,j,l} d_{ij} d_{jl} e_{li}/N$, respectively. Technically, we have

$$p^{(1,1)} = \frac{\mathbf{tr}(\mathbf{M}_I \mathbf{M}_R)}{N}, \qquad p^{(2,1)} = \frac{\mathbf{tr}(\mathbf{M}_I^2 \mathbf{M}_R)}{N},$$

where $\mathbf{M}_I$ ($\mathbf{M}_R$) denotes the adjacency matrix of G_I (G_R) and $\mathbf{tr}(\mathbf{M})$ presents the trace of matrix $\mathbf{M}$, i.e., the sum of diagonal entries in $\mathbf{M}$.

§2. A unifying formula to predict $\rho_C > \rho_D$ in a class of spatial structures

Here we investigate a class of spatial structures that both interaction and dispersal graphs are unweighted while not necessarily symmetric. When interaction and dispersal graphs are unweighted and symmetric, we recover spatial structures used in most prior studies. Furthermore, we provide two variations of public goods games in these spatial structures, i.e., random public goods games and l-order public goods games (see Results section in the main text for details). These two variations greatly extend the research scope of multiplayer games in structured populations. They can also recover the conventional spatial public goods game as a special case by taking $L = k_I + 1$ in random public goods games or $l = 1$ in l-order public goods games. Analytical results for public goods games on unweighted graphs can de derived from §1. N-evertheless, if we do so, we probably miss many important findings and it is also difficult to generalize such results to the two variations. In this section, we provide an alternative approach to get an analytical condition and then show that it is applicable in various spatial structures and variations.

We first introduce two concepts, (i) interaction partner and (ii) role model. Players who can interact with player i in some games (regardless of the organizers) are i's interaction partners. That is, if player i and j are likely to participate in the same game, they are interaction partner of each other. We designate Ω_I^i to be the set of i's interaction partners. For example, in well-mixed settings Ω_I^i includes all players except i. In the aforementioned structured populations, both the first-order (nearest) and second-order (next nearest) neighbours in the interaction graph are i's interaction partners. Players whose offspring potentially occupy node i or who could disperse strategies to player i are termed i's role models. Let Ω_R^i denote the set of i role models and $|\Omega_R^i|$ the number of role models. In the dispersal graph, $|\Omega_R^i|$ corresponds to the node degree k_R. Note that Ω_I^i and Ω_R^i are not necessarily identical.

Conventional spatial public goods game

A public goods game with L participants and an enhancement factor r actually can be decomposed into $L(L-1)/2$ two-player games with a payoff matrix

$$\begin{array}{ll} & \begin{array}{cc} \text{Cooperate} & \text{Defect} \end{array} \\ \begin{array}{l} \text{Cooperate} \\ \text{Defect} \end{array} & \begin{pmatrix} \frac{r-1}{L-1} & \frac{r-L}{L(L-1)} \\ \frac{r}{L} & 0 \end{pmatrix} \end{array}.$$

Accordingly, from the perspective of two-player games, each player plays such a two-player game with other $L-1$ participants, respectively. Then we transform the conventional spatial public goods games to spatial two-player games. Concretely, we decompose each public goods game into $L(L-1)/2$ two-player games and construct a new interaction graph to describe the games. If player i and j play two-player games, we build an edge between them. Let n_j^i denote the interaction times that i plays two-player games with j. Actually, n_j^i is also the number of PGGs in which i and j participate concurrently before decomposition. Note that before decomposition each player participates in L L-player public goods game in each generation. After decomposition, each player thus plays $L(L-1)$ two-player games in each generation. Thus i interacts with j at a frequency $n_j^i/[L(L-1)]$. We endow the interaction edge between i and j with a weight $\widetilde{d}_{ij} = n_j^i/[L(L-1)]$. Implementing this operation for all node pairs, we finally generates a new interaction graph for two-player games. Note that the strategy dispersal graph remains unchanged. Under two-player games, i's payoff in the interaction with j is

$$\widetilde{f}_j^i = \widetilde{d}_{ij} L(L-1)\left[\frac{r-1}{L-1}s_i s_j + \frac{r-L}{L(L-1)}s_i(1-s_j) + \frac{r}{L}(1-s_i)(1-s_j)\right]. \tag{S14}$$

s_i is i's strategy and s_j is j's strategy, where $s_i = 1$ means cooperation and $s_i = 0$ defection. The transformation from multiplayer public goods games to two-player games does not affect the evolutionary dynamics. Especially, the newly generated interaction graph and dispersal graph are still joint transitive and $\sum_{j\in V}\widetilde{d}_{ij} = 1$. We introduce a parameter called "assortment coefficient"

$$\theta = \frac{\sum_{j\in\Omega_R^i} n_j^i}{\sum_{j\in\Omega_I^i} n_j^i}\frac{1}{|\Omega_R^i|}. \tag{S15}$$

$\sum_{j\in\Omega_R^i} n_j^i$ represents the sum of times that i interacts with each role model, denoted by n_R. $\sum_{j\in\Omega_I^i} n_j^i$ represents the sum of times that i interacts with each interaction partner, denoted by n_I. Combining $|\Omega_R^i| = k_R$ and rewriting equation (S15) with n_R, n_I, we have equation (3.1) in the main text.

Furthermore $\sum_{j\in\Omega_I^i} n_j^i = L(L-1)$ and thus $n_j^i/\sum_{j\in\Omega_I^i} n_j^i = \widetilde{d}_{ij}$. In fact, θ maps the probability that a random walk with one step in the newly generated interaction graph and one step in the dispersal graph terminates in the starting node. Thus θ corresponds to $p^{(1,1)}$ in reference [3]. Here we stress that $p^{(1,1)}$ corresponds to the quantity in the new interaction and original dispersal graph. We further rewrite equation (S14) as

$$\widetilde{f}_j^i = \widetilde{d}_{ij}\left[L(r-1)s_i s_j + (r-L)s_i(1-s_j) + r(L-1)(1-s_i)(1-s_j)\right].$$

Thus the public goods games on graphs are equivalent to the two-player games on newly generated graphs and the payoff structure is

$$\begin{array}{ll} & \begin{array}{cc}\text{Cooperate} & \text{Defect}\end{array} \\ \begin{array}{l}\text{Cooperate}\\ \text{Defect}\end{array} & \begin{pmatrix} L(r-1) & r-L \\ r(L-1) & 0 \end{pmatrix}. \end{array}$$

Substituting θ and payoff values into equation (20) in Ref. [3], we have

$$r^* = \frac{(N-2)L}{N(L-1)\theta + N - 2L}. \tag{S16}$$

Furthermore, we provide a formula to calculate θ. Let $\mathbf{M}_I$ denote the adjacency matrix of the original interaction graph, where the entry in the i_{th} row and the j_{th} column is $1/k_I$ if there is an edge between node i and j, and 0 if not. $\mathbf{M}_R$ denotes the adjacency matrix of the dispersal graph, where the value in the i_{th} row and the j_{th} column is $1/k_R$ if there is a link between node i and j, and 0 if not. We focus on player i to calculate how many times it interacts with its role models. In fact, only when a role model j overlaps a player within a 2-step walk from i in the interaction graph, $n_j^i > 0$. If j is the nearest neighbour of i, i encounters j in both i-centred and j-centred PGGs, corresponding to $2k_I k_R d_{ij} e_{ji}$. If j and i have n neighbours in common, i encounters j in PGGs centred on each common neighbour, corresponding to $\sum_{l\in V} k_I^2 k_R d_{il} d_{lj} e_{ji}$. Enumerating all cases, we have

$$\begin{aligned}\sum_{j\in\Omega_R^i} n_j^i &= \sum_{j\in V} 2k_I k_R d_{ij} e_{ji} + \sum_{j,l\in V} k_I^2 k_R d_{il} d_{lj} e_{ji} \\ &= \frac{2k_I k_R \mathbf{tr}(\mathbf{M}_I\mathbf{M}_R) + k_I^2 k_R \mathbf{tr}(\mathbf{M}_I^2\mathbf{M}_R)}{N}\end{aligned} \tag{S17}$$

where $\mathbf{tr}(\mathbf{M})$ is the sum of all diagonal elements in $\mathbf{M}$. Substituting equation (S17) into equation (S15) and combining $L = k_I + 1$, we have

$$\theta = \frac{2\mathbf{tr}(\mathbf{M}_I\mathbf{M}_R) + k_I\mathbf{tr}(\mathbf{M}_I^2\mathbf{M}_R)}{N(k_I+1)}. \tag{S18}$$

l-order public goods game on graphs.

Any l-order PGG on graphs can be reduced to the conventional PGG on graphs by revising the interaction graph (see figure S3): connecting all nodes within a l-step walk to the node occupied by the focal player; revising all edge weights from $1/k_I$ to $1/\tilde{k}_I$, where $\tilde{k}_I$ is the node degree in the newly generated interaction graph. After the reduction, we analyse the conventional PGG in the spatial structure described by the new interaction and original dispersal graph.

Here we make a brief instruction to present that the reduction does not affect evolutionary dynamics. For player i, in l-order PGG on graphs, it participates in games centred on itself and all players within a l-step walk from i. In the reduced version, all these players within a l-step walk are connected to i and thus i is also engaged in games centred on them in terms of the conventional PGG on graphs. Analogously, all participants in a l-order PGG centred on player i are also participants in the reduced PGG centred on player i. Thus, the reduction remains players' payoffs unchanged. Besides, the reduction is independent of the dispersal graph. To use results obtained in the conventional PGG on graphs, i.e., equations (S15), (S16), (S17), and (S18), we normalized all edge weights in newly generated interaction graph to $1/\tilde{k}_I$ such that the sum of edge weights associated with a node is 1.

Let $\mathbf{M}_I$ and $\mathbf{M}_R$ denote the adjacency matrix of the interaction graph and the dispersal graph in l-order PGG, respectively. Let $\widetilde{\mathbf{M}}_I$ denote the adjacency matrix of the interaction graph in reduced l-order PGG. We introduce a matrix operator $[\bullet]$, which makes $[\mathbf{M}]_{ij} = 1$ if $M_{ij} \neq 0$ and $[\mathbf{M}]_{ij} = 0$ if $M_{ij} = 0$, where $M_{ij}(\widetilde{M_{ij}})$ is the entry of $\mathbf{M}$ ($\widetilde{\mathbf{M}}$) in row i and column j. Then we get

$$\tilde{k}_I = \frac{\mathbf{e}^{\mathrm{T}}\left[\sum_{i=0}^{l}\mathbf{M}_I^i\right]\mathbf{e}}{N} - 1,$$

where $\mathbf{M}^0$ is a N-by-N identity matrix $\mathbf{I}$ and $\mathbf{e}$ is an identity column vector with N elements. $\widetilde{\mathbf{M}}_I$ is given by

$$\widetilde{\mathbf{M}}_I = \frac{N\left(\left[\sum_{i=0}^{l}\mathbf{M}_I^i\right] - \mathbf{I}\right)}{\mathbf{e}^{\mathrm{T}}\left[\sum_{i=0}^{l}\mathbf{M}_I^i\right]\mathbf{e} - N}. \tag{S19}$$

Combining equation (S18), in l-order PGG, we have

$$\theta = \frac{2\mathbf{tr}(\widetilde{\mathbf{M}}_I\mathbf{M}_R) + \tilde{k}_I\mathbf{tr}(\widetilde{\mathbf{M}}_I^2\mathbf{M}_R)}{N(\tilde{k}_I+1)}.$$

Random public goods game on graphs.

Random PGG on graphs helps to confirm the generality of the unifying formula, ranging from two-player games to the collective interaction in well-mixed settings. Under the random PGG, for each player, the number of the focal player and its neighbours exceeds the PGG size, $k_I+1 >$

L. Thus in each PGG, the participants include the focal player and $L-1$ randomly selected neighbours. Note that the sum of interaction times that all players interact with the focal player is still $L(L-1)$. Here we stress the interaction times under random public goods games are different from those in conventional spatial public goods games. For example, if player i and j are connected to each other, in i-centred games, j is selected to be a participant with probability $\binom{k_I-1}{L-2}/\binom{k_I}{L-1}$ rather than 1 in the conventional spatial public goods games. Equivalently, player j interacts with i for $\binom{k_I-1}{L-2}/\binom{k_I}{L-1}$ times in i-centred game. If player i and j have a common neighbour, the probability that both i and j are selected to be the participants is $\binom{k_I-2}{L-3}/\binom{k_I}{L-1}$. Thus, in a PGG centred on the common neighbour, i and j interact for $\binom{k_I-2}{L-3}/\binom{k_I}{L-1}$ times. Overall, we have

$$\begin{aligned}\sum_{j\in\Omega_R^i} n_j^i &= \sum_{j\in V} 2k_I k_R d_{ij} e_{ji} \frac{\binom{k_I-1}{L-2}}{\binom{k_I}{L-1}} + \sum_{j,l\in V} k_I^2 k_R d_{il} d_{lj} e_{ji} \frac{\binom{k_I-2}{L-3}}{\binom{k_I}{L-1}} \\ &= \frac{2(L-1)k_R \mathbf{tr}(\mathbf{M}_I\mathbf{M}_R) + k_I k_R \mathbf{tr}(\mathbf{M}_I^2\mathbf{M}_R)\frac{(L-1)(L-2)}{(k_I-1)}}{N}\end{aligned}$$

and

$$\theta = \frac{2(k_I-1)\mathbf{tr}(\mathbf{M}_I\mathbf{M}_R) + k_I(L-2)\mathbf{tr}(\mathbf{M}_I^2\mathbf{M}_R)}{NL(k_I-1)}.$$

§3. Emergence of spatial reciprocity

We use subscripts "spa" and "wel" to indicate the quantity obtained in spatial structures and well-mixed settings, respectively. According to equation (S16), a spatial structure favours cooperation only when the assortment coefficient in the spatial structure (θ_{spa}) is larger than the assortment coefficient in the well-mixed setting (θ_{wel}), where $\theta_{\text{wel}} = 1/(N-1)$. According to equation (S15), $\theta_{\text{spa}} > \theta_{\text{wel}}$ means

$$\frac{n_R}{n_I}\frac{1}{k_R} > \frac{1}{N-1}. \tag{S20}$$

We stress that n_R, n_I, and k_R depend on the local spatial arrangement and are independent of the population size N. As long as $n_R > 0$, inequation (S20) holds for sufficiently large population size N. The minimum population size is $N^* = 2 + L(L-1)k_R/n_R$. $n_R > 0$ means that there are role models overlapping interaction partners. Under the conventional spatial public goods games, when a role model overlaps an interaction partner, it interacts with the focal player at least once. Therefore we have $n_R \geq 1$. In particular, when this role model overlaps a next nearest neighbour (in the interaction graph) who has only one common neighbour with the focal player, the interaction time of this role model with the focal player is 1. Then we have

$$N^* = 2 + k_I(k_I+1)k_R.$$

Analogously, we can derive the the minimum population size under random public goods games and l-order public goods games. Under the random public goods games, in each generation, the expected interaction times of an interaction parter with the focal player are at least $\binom{k_I-2}{L-3}/\binom{k_I}{L-1}$. If there are role models overlapping interaction partners, $n_R \geq \binom{k_I-2}{L-3}/\binom{k_I}{L-1}$. We have the minimum population size

$$N^* = 2 + \frac{k_I(k_I-1)k_R L}{L-2}.$$

Especially, for $L = 2$, we have $N^* = 2 + k_I k_R$. Under l-order public goods games, when overlapping an interaction partner, the role model interacts with the focal player at least once. We have the minimum population size

$$N^* = 2 + L(L-1)k_R.$$

If no role models overlap interaction partners, we have $n_R = 0$ and $\theta_{\text{spa}} = 0$. This leads to the most testing environment for the evolution of cooperation. That is,

$$n_R = 0 \Longrightarrow r^*_{\text{spa}} > r^*_{\text{wel}}.$$

§4. Enhancement of spatial reciprocity

Equation (S16) suggests that for two spatial structures (structure 1 and structure 2) that only differ in connections (have the same population size and node degrees),

$$r_1^* < r_2^* \Longleftrightarrow n_{R_1} > n_{R_2}. \tag{S21}$$

where r_1^* (r_2^*) denotes the critical enhancement factor for cooperation winning defection and n_{R_1} (n_{R_2}) denotes the sum of times that a player interacts with each of its role model in spatial structure 1 (2). In particular, if fixing the interaction graph G_I, we can get such a corollary: for any focal player and two other different players j_1 and j_2,

$$r^*_{j_1\in\Omega_R, j_2\notin\Omega_R} < r^*_{j_1\notin\Omega_R, j_2\in\Omega_R} \Longleftrightarrow n_{j_1} > n_{j_2}, \tag{S22}$$

where $j_1 \in \Omega_R, j_2 \notin \Omega_R$ means that the focal player takes j_1 but not j_2 to be the role model. Intuitively, for any player i, if i interacts with j_1 for more times than with j_2, i choosing j_1 as the role model brings more benefits to cooperation than choosing j_2. Thus, relying on local interaction information, players can enhance spatial reciprocity by adjusting their own role models.

Similarly, if fixing role models (fixing G_R), players can also adjust interaction partners to enhance spatial reciprocity. Compared with adjusting role models, adjusting interaction partners is more complicated. Due to the complexity of group interactions, adjusting an interaction partner may change interaction times of the focal player with many other players, which is hard to be accurately captured by a simple rule. However, we still give some insightful views based on equation (S22). First we put forward a proposition like below:

Proposition In a pair of symmetric interaction and dispersal graphs, for $j \in \Omega_I^i$ and $j' \notin \Omega_I^i$,

$$n_R^i < n_{R'}^i \Longleftrightarrow n_j^i < n_{j'}^i, \tag{S23}$$

where n_R^i ($n_{R'}^i$) represents the sum of interaction times that i interacts with each of its role models before (after) i rewires the interaction edge from j to j', and n_j^i ($n_{j'}^i$) is the interaction times of i with j (j') before rewiring the interaction edge. In other words, if i interacts with j' more times than with j, i breaking the interaction edge with j and then rewiring it to j' will increase i's total interaction times with its role models.

Proof Let $\mathbf{M}_I$ ($\mathbf{M}_{I'}$) denote the adjacency matrix of G_I before (after) the rewiring process. n_R^i

is given by

$$
\begin{aligned}
&\frac{n_R^i}{2k_I} = \sum_{m\in\Omega_R^i} \left[\frac{k_I}{2}\left(\mathbf{M}_I\right)_{im}^2 + \left(\mathbf{M}_I\right)_{im}\right] \\
&= \left[\frac{k_I}{2}\left(\mathbf{M}_I\right)_{ij}^2 + \left(\mathbf{M}_I\right)_{ij}\right] + \sum_{m\in\Omega_R^i|j} \left[\frac{k_I}{2}\left(\mathbf{M}_I\right)_{im}^2 + \left(\mathbf{M}_I\right)_{im}\right] \\
&= \left[\frac{k_I}{2}\left(\mathbf{M}_I\right)_{ij}^2 + \left(\mathbf{M}_I\right)_{ij}\right] + \sum_{m\in\Omega_R^i|j} \left[\frac{k_I}{2}\left(\mathbf{M}_I\right)_{ij}\left(\mathbf{M}_I\right)_{jm} + \frac{k_I}{2}\left(\mathbf{M}_I\right)_{ij'}\left(\mathbf{M}_I\right)_{j'm}\right. \\
&\quad \left. + \frac{k_I}{2}\sum_{z\neq j,j'}\left(\mathbf{M}_I\right)_{iz}\left(\mathbf{M}_I\right)_{zm} + \left(\mathbf{M}_I\right)_{im}\right] \\
&= \left[\frac{k_I}{2}\left(\mathbf{M}_I\right)_{ij}^2 + \left(\mathbf{M}_I\right)_{ij}\right] + \sum_{m\in\Omega_R^i|j} \left[\frac{k_I}{2}\left(\mathbf{M}_I\right)_{ij}\left(\mathbf{M}_I\right)_{jm}\right. \\
&\quad \left. + \frac{k_I}{2}\sum_{z\neq j,j'}\left(\mathbf{M}_I\right)_{iz}\left(\mathbf{M}_I\right)_{zm} + \left(\mathbf{M}_I\right)_{im}\right].
\end{aligned} \tag{S24}
$$

$n_{R'}^i$ is given by

$$
\begin{aligned}
&\frac{n_{R'}^i}{2k_I} = \sum_{m\in\Omega_R^i} \left[\frac{k_I}{2}\left(\mathbf{M}_{I'}\right)_{im}^2 + \left(\mathbf{M}_{I'}\right)_{im}\right] \\
&= \left[\frac{k_I}{2}\left(\mathbf{M}_{I'}\right)_{ij}^2 + \left(\mathbf{M}_{I'}\right)_{ij}\right] + \sum_{m\in\Omega_R^i|j} \left[\frac{k_I}{2}\left(\mathbf{M}_{I'}\right)_{im}^2 + \left(\mathbf{M}_{I'}\right)_{im}\right] \\
&=\frac{k_I}{2}\left(\mathbf{M}_{I'}\right)_{ij}^2 + \sum_{m\in\Omega_R^i|j} \left[\frac{k_I}{2}\left(\mathbf{M}_{I'}\right)_{ij}\left(\mathbf{M}_{I'}\right)_{jm} + \frac{k_I}{2}\left(\mathbf{M}_{I'}\right)_{ij'}\left(\mathbf{M}_{I'}\right)_{j'm}\right. \\
&\quad \left. + \frac{k_I}{2}\sum_{z\neq j,j'}\left(\mathbf{M}_{I'}\right)_{iz}\left(\mathbf{M}_{I'}\right)_{zm} + \left(\mathbf{M}_{I'}\right)_{im}\right] \\
&=\frac{k_I}{2}\left(\mathbf{M}_I\right)_{ij}^2 + \frac{k_I}{2}\frac{1}{k}\left(\mathbf{M}_I\right)_{j'j} + \sum_{m\in\Omega_R^i|j} \left[\frac{k_I}{2}\frac{1}{k}\left(\mathbf{M}_I\right)_{j'm}\right. \\
&\quad \left. + \frac{k_I}{2}\sum_{z\neq j,j'}\left(\mathbf{M}_I\right)_{iz}\left(\mathbf{M}_I\right)_{zm} + \left(\mathbf{M}_I\right)_{im}\right].
\end{aligned} \tag{S25}
$$

Combining Eqs. (S24) and (S25), we have

$$
\begin{aligned}
&\frac{n_R^i}{2k_I} - \frac{n_{R'}^i}{2k_I} \\
=&\left(\mathbf{M}_I\right)_{ij} + \sum_{m\in\Omega_R^i|j} \frac{k_I}{2}\left(\mathbf{M}_I\right)_{ij}\left(\mathbf{M}_I\right)_{jm} - \frac{k_I}{2}\frac{1}{k}\left(\mathbf{M}_I\right)_{j'j} - \sum_{m\in\Omega_R^i|j} \frac{k_I}{2}\frac{1}{k}\left(\mathbf{M}_I\right)_{j'm} \\
=&\left(\mathbf{M}_I\right)_{ij} + \sum_{m\in\Omega_R^i} \frac{k_I}{2}\left(\mathbf{M}_I\right)_{im}\left(\mathbf{M}_I\right)_{mj} - \frac{k_I}{2}\left(\mathbf{M}_I\right)_{ij}\left(\mathbf{M}_I\right)_{jj'} - \sum_{m\in\Omega_R^i|j} \frac{k_I}{2}\left(\mathbf{M}_I\right)_{im}\left(\mathbf{M}_I\right)_{mj'} \\
=&\left[\frac{k_I}{2}\left(\mathbf{M}_I\right)_{ij}^2 + \left(\mathbf{M}_I\right)_{ij}\right] - \left[\frac{k_I}{2}\left(\mathbf{M}_I\right)_{ij'}^2 + \left(\mathbf{M}_I\right)_{ij'}\right] \\
=&\frac{1}{2k_I}(n_j^i - n_{j'}^i)
\end{aligned}
$$

Thus, $n_R^i - n_{R'}^i = n_j^i - n_{j'}^i$. ■

However, we have to point that equation (S23) is valid on the assumption that only i adjusts its interaction edge. If other players implement the same procedure, the set of i's interaction partners probably changes dramatically, which makes it hard to provide an exact analytic result. Intriguingly, we can still take advantages of equations (S22) and (S23) to develop an algorithm to enhance spatial reciprocity. In this algorithm, just relying on local interaction information (interaction partners, interaction times, and role models), players adjust their interaction edges or dispersal edges. The algorithm starts from a pair of symmetric interaction and dispersal graphs. The detailed steps are

(1) Randomly choose a player i and record the interaction times of i with each interaction partner.

(2) For player j_1 (connected to i in the interaction graph) and j_2 (not connected to i in the interaction graph), if i interacts more times with j_2 than with j_1, i breaks its interaction edge with j_1 and builds an edge to j_2. Otherwise the algorithm terminates.

(3) Player i rewires the dispersal edge from j_1 to j_2, and the algorithm returns to step (1).

To keep node-transitivity, all players implement the same rewiring operation simultaneously. This algorithm has been proved to effectively enhance spatial reciprocity in most cases (see figure S4).

§5. Structural clusters

Real-world spatial structures are usually highly clustered [5]. Here we refer to dense triangle loops and a high global clustering coefficient $\mathcal{C}$, defined to be [5]

$$\mathcal{C} = \frac{3 \times \text{number of triangle loops}}{\text{number of connected triplets of nodes}}.$$

For a node i with degree k_I, its local clustering coefficient is defined as

$$\mathcal{C}_i = \frac{\text{number of triangle loops with } i}{\text{number of connected triplets of } i}, \tag{S26}$$

where the denominator is given by $k_I(k_I - 1)/2$. In joint transitive graphs, the local clustering coefficient equals to the global clustering coefficient, i.e., $\mathcal{C} = \mathcal{C}_i$. In symmetric interaction and dispersal graphs ($k_I = k_R = k$), $p^{(2,1)}$ is equivalent to the probability that a three-step random walk in G_I terminates in the starting point. Since there are no self-loops, such a random walk must go through a triangle loop, and the corresponding probability is $1/k^3$. Thus, the total number of triangle loops associated with a node is $p^{(2,1)}/(2/k^3)$, where factor 2 in the denominator results from different directions of the first step in such a three-step random walk, i.e., $i \to j_1 \to j_2 \to i$ and $i \to j_2 \to j_1 \to i$. Altogether, the clustering coefficient is given by

$$\mathcal{C}_i = \frac{p^{(2,1)}k^3/2}{k(k-1)/2} = \frac{p^{(2,1)}k^2}{k-1}. \tag{S27}$$

We replace $\mathcal{C}_i$ with $\mathcal{C}$. Substituting equation (S27) into equations (S9), (S11), and (S13), we can get

$$r^* = \begin{cases} \frac{(N-1)(k+1)}{N-(k+1)} & \text{BD/PC} \\ \frac{(k+1)^2(N-2)}{N[k+3+(k-1)\mathcal{C}]-2(k+1)^2} & \text{DB} \\ \frac{N(k+1)^2(k+2)-2(k+1)^3}{N[k^2+5k+2+k(k-1)\mathcal{C}]-2(k+1)^3} & \text{IM} \end{cases} \tag{S28}$$

In addition, in the symmetric and unweighted interaction and dispersal graphs, from equation (S18), we have

$$\mathcal{C} = \frac{(k+1)k\theta - 1}{k-1}. \tag{S29}$$

Next, we present results for four typical graphs illustrated in figure S2 under the death-birth update rule (results under other updates can be obtained in an analogous way).

Group-structured graph (M is the number of group)

For $M = 3$

$$p^{(2,1)} = \frac{k^2 - 5k + 8}{k^3}, \quad \mathcal{C} = \frac{k^2 - 5k + 8}{k(k-1)},$$
$$r^* = \frac{k(k+1)^2(N-2)}{2(k^2 - k + 4)N - 2k(k+1)^2} \xrightarrow{N \gg 1} r^* = \frac{k(k+1)^2}{2(k^2 - k + 4)}.$$

For $M > 3$

$$p^{(2,1)} = \frac{(k-2)(k-3)}{k^3}, \quad \mathcal{C} = \frac{(k-2)(k-3)}{k(k-1)},$$
$$r^* = \frac{k(k+1)^2(N-2)}{2(k^2 - k + 3)N - 2k(k+1)^2} \xrightarrow{N \gg 1} r^* = \frac{k(k+1)^2}{2(k^2 - k + 3)}.$$

Cycle

$$
\begin{aligned}
p^{(2,1)} &= \frac{3(k-2)}{4k^2}, \quad \mathcal{C} = \frac{3(k-2)}{4(k-1)}, \\
r^* &= \frac{4(k+1)^2(N-2)}{(7k+6)N - 8(k+1)^2} \xrightarrow{N \gg 1} r^* = \frac{4(k+1)^2}{(7k+6)}.
\end{aligned} \tag{S30}
$$

Lattice

$$
\begin{aligned}
p^{(2,1)} &= 0, \quad \mathcal{C} = 0, \quad r^* = \frac{8(N-2)}{3N-16} \xrightarrow{N \gg 1} r^* = \frac{8}{3} \quad (k=3). \\
p^{(2,1)} &= 0, \quad \mathcal{C} = 0, \quad r^* = \frac{25(N-2)}{7N-50} \xrightarrow{N \gg 1} r^* = \frac{25}{7} \quad (k=4). \\
p^{(2,1)} &= \frac{1}{18}, \quad \mathcal{C} = \frac{2}{5}, \quad r^* = \frac{49(N-2)}{11N-98} \xrightarrow{N \gg 1} r^* = \frac{49}{11} \quad (k=6). \\
p^{(2,1)} &= \frac{3}{64}, \quad \mathcal{C} = \frac{3}{7}, \quad r^* = \frac{81(N-2)}{14N-162} \xrightarrow{N \gg 1} r^* = \frac{81}{14} \quad (k=8).
\end{aligned}
$$

Random k-regular graph For the random k-regular graph (random regular graph with average degree k), the number of triangle loops is asymptotically Poisson random variable with mean [10]

$$
\lambda = \frac{(k-1)^3}{6}.
$$

For sufficiently large N, the clustering coefficient and critical enhancement factor can be derived as

$$
\begin{aligned}
p^{(2,1)} &= \frac{(k-1)^3}{3Nk^3}, \quad \mathcal{C} = \frac{(k-1)^2}{3Nk}, \\
r^* &= \frac{(k+1)^2(N-2)}{N(k+3) + \frac{(k-1)^3}{3k} - 2(k+1)^2} \xrightarrow{N \gg 1} r^* = \frac{(k+1)^2}{(k+3)}
\end{aligned} \tag{S31}
$$

The last term recovers the result obtained in a previous work [11].

§6. Heterogeneous social ties

Self participation frequency w**.** For a given spatial structure with a sufficiently large size ($N \gg 1$), r^* is a function of w, noted $r^*(w)$.

Under BD/PC update rule, based on equation (S9), we get the extreme point of $r^*(w)$, $w = 1/(\kappa+1)$, which is located in the range $[0,1]$. Thus $r^*(w)$ is a non-monotonic function of w. The representative points for $r^*(w)$ are given by

$$r^*(w) = \begin{cases} \kappa & w = 0 \\ \kappa+1 & w = \frac{1}{\kappa+1} \\ 1 & w = 1 \end{cases}$$

Under DB update rule, based on equation (S11), we get the extreme point of $r^*(w)$,

$$w = \frac{\kappa^{-1} + p^{(2,1)} - p^{(1,1)}}{1 + \kappa^{-1} + p^{(2,1)} - 2p^{(1,1)}}. \tag{S32}$$

Its denominator is positive since

$$\begin{aligned} & 1 + \kappa^{-1} + p^{(2,1)} - 2p^{(1,1)} \\ \geq & 1 + \sum_{j \in N_i^I} d_{ij}^2 - 2\sum_{j \in N_i^I} d_{ij} e_{ij} \\ \geq & 1 + \sum_{j \in N_i^I} d_{ij}^2 - 2max\{d_{ij}\}_{j \in N_i^I} \\ \geq & (1 - max\{d_{ij}\}_{j \in N_i^I})^2 \\ \geq & 0. \end{aligned}$$

The equality holds only when each node has only one edge in both interaction graph and dispersal graph and meanwhile they coincide. Evidently, such graphs are not connected and the fixation probability for the mutant strategy is zero. If the spatial structure makes $p^{(1,1)} < \kappa^{-1} + p^{(2,1)}$, $r^*(w)$ is a non-monotonic function of w. The representative points for $r^*(w)$ are given by

$$r^*(w) = \begin{cases} \frac{\kappa}{1+\kappa p^{(2,1)}} & w = 0 \\ \frac{\kappa^{-1}+p^{(2,1)}-2p^{(1,1)}+1}{\kappa^{-1}+p^{(2,1)}-(p^{(1,1)})^2} & w = \frac{\kappa^{-1}+p^{(2,1)}-p^{(1,1)}}{1+\kappa^{-1}+p^{(2,1)}-2p^{(1,1)}} \\ 1 & w = 1 \end{cases}$$

However, if $p^{(1,1)} \geq \kappa^{-1} + p^{(2,1)}$, $r^*(w)$ decreases monotonously as the increasing w from 0 to 1 and reaches to 1 for $w = 1$.

Under IM update rule, based on equation (S13), the extreme point of $r^*(w)$ is

$$w = \frac{k_I^{-1} + \tilde{p}^{(2,1)} - \tilde{p}^{(1,1)}}{1 + k_I^{-1} + \tilde{p}^{(2,1)} - 2\tilde{p}^{(1,1)}}, \tag{S33}$$

where $\tilde{p}^{(1,1)} = k_R p^{(1,1)}/(k_R+2)$ and $\tilde{p}^{(2,1)} = k_R p^{(2,1)}/(k_R+2)$. As demonstrated above, the denominator is positive. Similarly, the numerator is positive since $\tilde{p}^{(1,1)} < p^{(1,1)} = \sum_{j \in N_I^R} 1/(k_I k_R) < 1/(k_I)$. Thus, $r^*(w)$ is a non-monotonic function of w. The representative points for $r^*(w)$ are given by

$$r^*(w) = \begin{cases} \frac{k_R}{1+k_R\tilde{p}^{(2,1)}} & w = 0 \\ \frac{k_I^{-1}+\tilde{p}^{(2,1)}-2\tilde{p}^{(1,1)}+1}{k_I^{-1}+\tilde{p}^{(2,1)}-(\tilde{p}^{(1,1)})^2} & w = \frac{k_I^{-1}+\tilde{p}^{(2,1)}-\tilde{p}^{(1,1)}}{1+k_I^{-1}+\tilde{p}^{(2,1)}-2\tilde{p}^{(1,1)}} \\ 1 & w = 1 \end{cases}$$

Strong social ties. The social tie between individual i and j is a strong social tie if in the interaction graph d_{ij} is larger than the average weight of all edges ($d_{ij} > 1/k_I$) and in the dispersal graph e_{ij} is larger than the average weight of all edges ($e_{ij} > 1/k_R$). We consider a baseline model where the interaction and dispersal graphs are identical and meanwhile all edges have the same weight ($k_I = k_R = k$). Introducing a strong tie between individual i and j means to increase d_{ij} and e_{ij}. In the baseline model, if introducing strong social ties reduces the threshold r^* for the success of cooperation, such strong social ties promote cooperation. But if the introduction of strong social ties gives rise to a larger r^*, such strong social ties inhibit cooperation. Here we investigate the death-birth rule.

First we study the spatial structure without structural clusters. Equation (S11) tells that r^* is negatively correlated to κ^{-1}, $p^{(1,1)}$, and $p^{(2,1)}$. Since there is no structural clusters, we have $p^{(2,1)} = 0$. We introduce strong ties in the baseline model by increasing the weights of a fraction of edges. Note that in both interaction and strategy dispersal graph, each node is linked to other k nodes by k edges. Let $\{1/k+\xi_1, 1/k+\xi_2, \cdots, 1/k+\xi_n\}$ denote weights of the k edges in the interaction graph after introducing strong social ties and $\{1/k+\sigma_1, 1/k+\sigma_2, \cdots, 1/k+\sigma_n\}$ denote weights of the k edges in the dispersal graph. Since the normalization of the sum of all edge weights, we have $\sum_{i=1}^{k}(1/k+\xi_i) = 1$ and $\sum_{i=1}^{k}(1/k+\sigma_i) = 1$, which gives $\sum_{i=1}^{k}\xi_i = 0$ and $\sum_{i=1}^{k}\sigma_i = 0$. A strong social tie (taking the i_{th} edge for example) means $\xi_i > 0$ and $\sigma_i > 0$. For other ties, $\xi_i \leq 0$ and $\sigma_i \leq 0$. Then we have $\kappa^{-1} = \sum_{i=1}^{k}(1/k+\xi_i)^2 = 1/k+\sum_{i=1}^{k}\xi_i^2 > 1/k$ and $p^{(1,1)} = \sum_{i=1}^{k}(1/k+\xi_i)(1/k+\sigma_i) = 1/k+\sum_{i=1}^{k}\xi_i\sigma_i > 1/k$. Thus, regardless of weights of the strong social ties, compared with the baseline model, introducing strong social ties always increases κ^{-1} and $p^{(1,1)}$. Thus, in spatial structures without structural clusters, strong social ties facilitate cooperation.

In spatial structures with structural clusters, we can use Eq (S11) to calculate the critical threshold r^* and then analyze how strong social ties affect the evolution of cooperation. The structural clusters make the conclusions complicated. For simplicity, we assume that each player has a strong social tie. Let d denote the weight of a strong interaction edge and $(1-d)/(k-1)$ the weight of other interaction edges. Let e denote the weight of a strong dispersal edge and then $(1-e)/(k-1)$ the weight of other dispersal edges. Note that if two players are linked by an interaction edge with $d > 1/k$ and a dispersal edge with $e > 1/k$, they own a strong social tie. Here we fix $w = 1/(k+1)$. Equation (S11) tells that $(1-w)^2\kappa^{-1}+w^2+2w(1-w)p^{(1,1)}+(1-w)^2p^{(2,1)}$ decides the value of r^*. Dividing it by $(1-w)^2$ and substituting $w = 1/(k+1)$, we have

$$\Phi(d,e) = \kappa^{-1} + \frac{2p^{(1,1)}}{k} + p^{(2,1)}$$

where $\kappa^{-1} = (kd^2-2d+1)/(k-1)$ and $p^{(1,1)} = (kde-d-e+1)/(k-1)$. $\Phi(d,e)$ is negatively correlated with the critical threshold r^*.

The spatial structure we studied is illustrated in the figure 4*b* in the main text and $k = 4$. We have

$$p^{(2,1)} = \frac{(d-1)(d+e+2de-4)}{27},$$

and

$$\Phi(d,e) = \frac{2d^2e}{27} + \frac{37d^2}{27} + \frac{17de}{27} - \frac{55d}{54} - \frac{11e}{54} + \frac{35}{54}.$$

Then, we get

$$
\begin{aligned}
\frac{\partial\phi}{\partial d} &= d\left[\frac{4e}{27}+\frac{74}{27}\right]+\left[\frac{17e}{27}-\frac{55}{54}\right], \\
\frac{\partial\phi}{\partial e} &= \frac{2d^2}{27}+\frac{17d}{27}-\frac{11}{54}.
\end{aligned}
$$

Since $\partial\phi/\partial d$ is negative for $d \in [1/4, (55-34e)/(148+8e))$ and $\partial\phi/\partial e$ negative for $e \in [1/4, (\sqrt{333}-17)/4)$, the increasing d and e in a certain range lead to a smaller $\phi(d,e)$ and a larger r^*. Thus in spatial structures with structural clusters, strong social edges might impede the evolution of cooperation.

About the study of strong social ties, our model is different from the prior work [3] in two ways:
(i) we consider the multiplayer game (prior work takes two-player game);
(ii) the strong tie in our work is a pair of interaction edge and dispersal edge and their weights are not necessarily identical (the strong tie in prior work is an edge using for both interaction and dispersal).
We stress that both multiplayer interactions and the separation of interaction edge and dispersal edge make the investigation complicated. Our work in this paper aims to provide a few theoretical insights into how these factors affect the collective cooperation. Meanwhile, it may be instrumental in designing mechanisms to leverage cooperation in multiagent systems.

§7. Practical social networks

In this paper, based on the jointly transitive graphs [3, 1, 2], we derive an exact condition to predict when natural selection favors cooperation over defection. A deep analysis into this condition provides a few new sights into many classical questions. Although jointly transitive graphs have covered a large class of classical spatial structures and have been widely used in theoretical studies [3, 1, 2]), to present the generality of our findings, we further investigate three practical social networks, i.e., homogeneous small-world network [4], Watts-Strogatz heterogeneous small-world network [5], and scale-free network [6, 12].

First, we show that the strength of spatial reciprocity is positively correlated to the sum of times that a player interacts with each role model [see Eq (3.3) in the manuscript]. Each player organizes a public goods game in which all neighbours and the organizer participate. Given that in heterogeneous networks n_R for each player (the sum of times that a player interacts with each role model) can be different, here we use the average value of n_R over all players, denoted by $\bar{n}_R$. In joint transitive graphs, we have $n_R = \bar{n}_R$. We consider three cases. That is, both interaction (G_I) and strategy dispersal (G_R) graphs are (i) homogeneous small-world networks, (ii) heterogeneous small-world networks, and (iii) scale-free networks. We consider two patterns to generate a spatial structure (described by a pair of networks) with tunable $\bar{n}_R$. Before introducing the two patterns, we present how to generate a single network. We build a single homogeneous small-world network based on the algorithm given in Ref. [4], the Watts-Strogatz heterogeneous small-world network based on Ref. [5], and the scale-free network based on growth and preferential attachment [12]. To present the first pattern (called 'edge swapping' pattern), we take the spatial structure described by a pair of homogeneous small-world networks for example:
(1) generate a single homogeneous small-world network for interaction and denote it by G_I [4];
(2) generate a copy of G_I and denote it by G_R;
(3) randomly select two edges of G_R and swap the ends of the two edges if no duplicate edges arise;
(4) repeat step (3) for h times.
We can adjust h to get pairs of homogeneous small-world networks with different $\bar{n}_R$s.
To present the second pattern (called 'node rearranging' pattern), we still take the spatial structure described by a pair of homogeneous small-world networks for example:
(1) generate a single homogeneous small-world network for interaction and denote it by G_I [4];
(2) label all nodes from 1 to N;
(3) generate a sequence $S_1 = \{1, 2, \cdots, N\}$, randomly select $\hat{N}$ labels in S_1 and rearrange the selected labels in their positions in a random way (positions of unselected labels remain unchanged), by which a new sequence S_2 is generated;
(4) generate G_R—if in G_I there exists an edge between node i and j, in G_R we build an edge between nodes whose labels appear in the i_{th} and j_{th} positions of S_2.
We can adjust $\hat{N}$ to get pairs of homogeneous small-world networks with different values of $\bar{n}_R$. Both 'edge swapping' and 'node rearranging' patterns ensure that both the interaction and strategy dispersal networks have the same node degree distribution. Besides, the 'node rearranging' pattern ensures that a few other structure properties such as clustering coefficients in the interaction and strategy dispersal networks are identical. Figure S7 shows that the larger $\bar{n}_R$ is, the smaller the critical enhancement factor r is, and the stronger the spatial reciprocity is. Thus, $\bar{n}_R$ is positively correlated to the strength of spatial reciprocity. Besides, in networks with small heterogeneity in node degrees, such as in homogeneous and heterogeneous small-world

networks, the analytical results (vertical lines) well predict when cooperation is favoured over defection (the cross points of dots and horizontal lines).

Next, we show in social networks, structural clusters act as an effective promotor of the evolution of cooperation (lines 220-221 in the main text). We consider three social networks (see figure S8 for more details). Figure S8 shows that the more structural clusters there are (the larger the clustering coefficient is), the smaller the critical enhancement factor is. Thus, structural clusters promote the evolution of cooperation.

Finally, we present in some cases strong social ties might inhibit cooperation (Section 4.2 in the main text). In the main text, we extend the public goods games in a pair of weighted and meanwhile joint transitive graphs (see Model section in the main text). We define the social tie between individual i and j to be a strong social tie if (i) in the interaction graph the weight of the edge connecting i and j is larger than the average weight of all edges; (ii) in the strategy dispersal graph the weight of edge connecting i and j is larger than the average weight of all edges. We find that introducing strong social ties does not always provide more advantages for cooperation. We provide a representative example, i.e., figure 4 in the main text. Here we further investigate the homogeneous small-world networks. We incorporate strong social ties into small-world networks using the algorithm illustrated in figure S9. Figure S10 shows that in such small-world networks, strong social ties lead to a higher critical enhancement factor. We have pointed out that the difference between the critical enhancement factors before and after introducing strong ties is small, predicted by the theoretical result shown in figure 4*c* in the main text.

Overall, our findings based on jointly transitive graphs hold in a few practical social networks. Although we can further extend the public goods games to any population structure, currently, it is greatly difficult to find an analytical result or explicit conclusions. We expect an enduring effort into this challenging work.

References

[1] F. Débarre, C. Hauert, and M. Doebeli. Social evolution in structured populations. *Nat. Commun.*, 5:3409, March 2014.

[2] Peter D. Taylor, Troy Day, and Geoff Wild. Evolution of cooperation in a finite homogeneous graph. *Nature*, 447(7143):469–472, May 2007.

[3] Benjamin Allen and Martin A. Nowak. Games on graphs. *EMS Surv. Math. Sci.*, 1:113–151, 2014.

[4] FC Santos, JF Rodrigues, and JM Pacheco. Epidemic spreading and cooperation dynamics on homogeneous small-world networks. *Phys. Rev. E*, 72(5, 2), NOV 2005.

[5] Duncan J. Watts and Steven H. Strogatz. Collective dynamics of 'small-world' networks. *Nature*, 393(6684):440–442, 1998.

[6] Petter Holme and Beom Jun Kim. Growing scale-free networks with tunable clustering. *Phys. Rev. E*, 65:026107, Jan 2002.

[7] Hisashi Ohtsuki, Christoph Hauert, Erez Lieberman, and Martin A. Nowak. A simple rule for the evolution of cooperation on graphs and social networks. *Nature*, 441(7092):502–505, 2006.

[8] C Hauert and M Doebeli. Spatial structure often inhibits the evolution of cooperation in the snowdrift game. *Nature*, 428(6983):643–646, 2004.

[9] Benjamin Allen, Jeff Gore, and Martin A. Nowak. Spatial dilemmas of diffusible public goods. *eLife*, 2:e01169, November 2013.

[10] Béta Bollobás. *Random Graphs*. Cambridge University Press, 2001.

[11] Aming Li, Bin Wu, and Long Wang. Cooperation with both synergistic and local interactions can be worse than each alone. *Sci. Rep.*, 4:5536, July 2014.

[12] Albert-László Barabási and Réka Albert. Emergence of scaling in random networks. *Science*, 286(5439):509–512, October 1999.